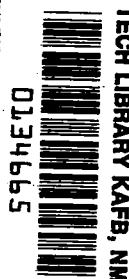


NASA Technical Paper 1491

NASA  
TP  
1491  
c.1



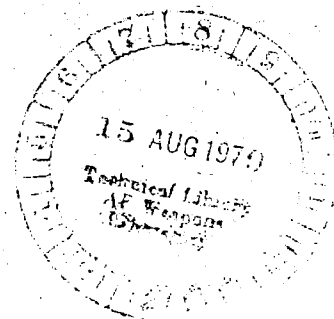
# Flow Visualization of Discrete-Hole Film Cooling With Spanwise Injection Over a Cylinder

Louis M. Russell

JULY 1979

LOAN COPY: RETURN TO  
AFWL TECHNICAL LIBRARY  
KIRTLAND AFB, N. M.

**NASA**





NASA Technical Paper 1491

# Flow Visualization of Discrete-Hole Film Cooling With Spanwise Injection Over a Cylinder

Louis M. Russell  
*Lewis Research Center*  
*Cleveland, Ohio*



National Aeronautics  
and Space Administration

**Scientific and Technical  
Information Branch**

1979

## SUMMARY

An investigation was conducted to provide insight into the fluid mechanics encountered when film air from a single row of holes is injected over a cylinder in a mainstream at conditions simulating a film-cooled, turbine-vane leading edge. Smoke was added to the cooling air to visualize its flow path. Film was injected in the spanwise direction at angles of  $30^\circ$  and  $45^\circ$  to the surface and angular locations of  $15^\circ$ ,  $30^\circ$ ,  $45^\circ$ , and  $60^\circ$  from the stagnation line. The tests were run at a mainstream Reynolds number based on the cylinder diameter of  $1.2 \times 10^5$  and a cylinder-diameter-to-cooling-hole-diameter ratio of 10.47. These conditions simulated those at the leading edge of an advanced turbine vane. Observations and photographs of the smoke in the injected stream were used to determine how various injection angles, cooling-hole locations, and blowing ratios (ratio of the mass flux of the injected stream to the mass flux of the local free stream) affected film flow path, film growth and spreading, film penetration through the boundary layer, and film departure from the surface. The observations are related to the measured heat-transfer data of others.

The results indicated that, in addition to the expected growth in film thickness and the greater penetration of the boundary layer with increasing blowing ratio, there was an absence of spanwise spreading and only a small spanwise deflection of the injected film. The film thicknesses were greater, at given blowing ratios, with injection from holes  $45^\circ$  to the surface than from holes  $30^\circ$  to the surface. Also the injected film tended to separate from the surface as the angular distance between the stagnation line and the injection location increased.

## INTRODUCTION

Increases in turbine-inlet temperature and pressure have reached the point where heat flux levels are too high for hot-section gas-turbine components to be adequately cooled by convection alone. Some film cooling is generally required to protect the metal parts from the hot gas stream. The most practical method currently used to film cool aircraft turbine blades and vanes is to inject the cooling air from discrete holes in their surfaces. It is important that the air be injected efficiently to provide the desired heat-transfer protection with a minimum disruption of the mainstream. Poorly designed film injection schemes can lead to mainstream momentum losses that severely reduce turbine aerodynamic efficiency (ref. 1) and, in some instances, even increase heat transfer to the surface (ref. 2). It is also important, for overall efficiency, to

minimize the amount of coolant used. One of the more difficult surfaces to cool is that at the leading edge.

Recent studies to determine the cooling effectiveness of injected cooling film on turbine-vane leading edges have used a cylinder in crossflow. Luckey, et al. (ref. 3) conducted experimental studies using a single row of spanwise holes at three injection angles and three angular injection locations relative to the stagnation line. Sasaki, et al. (ref. 4) obtained heat-transfer data with a rounded-leading-edge, flat-plate model. This model had four rows of holes at fixed angular injection locations relative to the stagnation line and at various injection angles relative to the surface in the spanwise direction. Both reports showed an improvement in cooling effectiveness as the injection angle relative to the surface was decreased, when injecting in the spanwise direction. The limited amount of flow visualization that was used in reference 4, showed primarily that high blowing ratios (injection-stream mass flux to mainstream mass flux) caused the injected flow to separate from the surface.

The investigation reported herein was conducted to provide further insight into the fluid mechanics encountered when film air is injected over a curved surface in a mainstream at conditions simulating a film-cooled, turbine-vane leading edge and to relate the observations to measured heat-transfer data. This should give a better understanding of the data trends.

In this study, smoke was added to the simulated cooling air to visualize its path. Film injection in the spanwise direction from a two-hole row was studied for two spanwise injection angles  $\beta$  ( $30^\circ$  and  $45^\circ$  to the surface) at four angular locations  $\theta$  ( $15^\circ$ ,  $30^\circ$ ,  $45^\circ$ , and  $60^\circ$ ) from the stagnation line and at various blowing ratios.

The tests were run with ambient-temperature air at a constant tunnel velocity of 15.5 meters per second. The mainstream Reynolds number based on the cylinder diameter was  $1.2 \times 10^5$ , and the ratio of cylinder diameter to cooling hole diameter was 10.47. The local blowing ratio  $M_L$  was varied from 0.21 to 3.50. Local blowing ratio is defined as the ratio of the mass flux (product of the density and velocity) of the injected stream to the mass flux of the local free stream.

The results are presented as a series of photographs of the smoke in the injected stream. Visual observations are also discussed. The results include the effect of various cooling-hole arrangements and blowing ratios on injectant flow path, film growth and spreading, film penetration through the boundary layer, and film departure from the surface. Also included are the heat-transfer performances inferred from the flow visualization and comparisons with the measured heat-transfer results of others. The turbulent structure of the injected flow could not be observed at the stream velocities required to maintain similitude for the tests herein. As a consequence, the influence of this turbulence on heat transfer could not be determined.

## APPARATUS AND PROCEDURE

### Apparatus

A schematic diagram of the test facility is shown in figure 1. It consisted of (1) a partially transparent plastic tunnel through which ambient-temperature air was drawn into a vacuum exhaust line, (2) a test section (in the tunnel) that included a cylinder with two film injection tubes, (3) a secondary air system that supplied the injected film air, (4) a smoke generator, (5) a plenum that served as a collection chamber for the smoke and the film air, and (6) a high-intensity quartz arc lamp that was used to illuminate the smoke.

The tunnel was 0.381 meter by 0.152 meter in cross section. The test section, shown in figure 2, consisted of a cylinder mounted on a 0.381-meter-by-0.61-meter plate. The cylinder was 11.43 centimeters in diameter and 15.24 centimeters high. Two metal delivery tubes were inserted inside the cylinder in the spanwise direction to represent film-cooling passages. The ends of these tubes were flush with the cylinder surface. The tubes were installed at an injection angle  $\beta$  of  $30^\circ$  (measured from the vertical in a plane through the cylinder and tube axes) for some tests and at an angle of  $45^\circ$  for other tests. The cylinder could be rotated about its axis to obtain the effect of injection at different angular locations  $\theta$  measured from the stagnation line. These angles,  $\beta$  and  $\theta$ , are referred to throughout this report. The inside diameter of the tubes was 1.09 centimeters and the length was 13.08 centimeters. The ratio of cylinder diameter to cooling-hole diameter was 10.47, typical of an advanced turbine vane.

The smoke generator, a schematic of which is shown in figure 3, was a commercially obtained device that used a heated mixture of carbon dioxide gas and mineral oil to produce an inert cloud of white smoke. This smoke was introduced through a rubber hose into the plenum below the test section to be mixed with the injection air.

### Procedure

Ambient-temperature air was used for both injected flow and mainstream flow. The free-stream velocity upstream of the test cylinder was 15.5 meters per second. This velocity was calculated from measurements of the total and static pressure. The free-stream turbulence intensity measured by a hot-wire probe was 2 percent. The free-stream Reynolds number  $Re$  based on the cylinder diameter was  $1.2 \times 10^5$ , which simulated the Reynolds number expected at the leading edge of advanced turbine vanes. Observations of the interaction of the injected flow with the mainstream were made at four angular locations  $\theta$  from the stagnation line of  $15^\circ$ ,  $30^\circ$ ,  $45^\circ$ , and  $60^\circ$  and at two spanwise injection angles  $\beta$  of  $30^\circ$  and  $45^\circ$ . Boundary-layer thicknesses  $\delta$  at each of

the four angular locations were calculated by using the Blasius solution for a laminar boundary layer (ref. 6). The thickness  $\delta$  is defined as the distance from the surface to the edge of the boundary layer, where the velocity is 98 percent of the free-stream velocity.

In the initial tests, helium-filled soap bubbles were used in the injected stream to visualize the flow, as done in reference 5. This method was not successful in the present study, however, because the bubble diameter ( $\sim 0.13$  cm) was larger than the boundary-layer thickness and, consequently, would not provide the desired information. The smoke generator apparatus was therefore used for the tests reported herein.

The mass flux of the injected stream was calculated from the continuity equation by dividing the sum of the measured mass flow rates of air and smoke by the total hole flow area. The injected-air mass flow rate was calculated from a rotameter reading. The smoke flow rate was determined by measuring the change in the weights of its constituents ( $\text{CO}_2$  and mineral oil) with time at a fixed pressure regulator setting on the smoke generator. This same regulator setting was used during the tests to maintain constant smoke flow rate. The mass flux of the mainstream was obtained from the product of the local mainstream velocity over the cylinder and the atmospheric air density. The local mainstream velocity was calculated from the measured tunnel mainstream velocity and the equation (ref. 6) for potential flow around a cylinder. The density was obtained from measured tunnel entrance temperature and barometric pressure since the pressure in the tunnel was essentially the same as room pressure.

Thirty-five-millimeter slide transparencies were taken to show the interaction between the injected film and the mainstream. Light reflections sometimes made good photographs difficult to obtain. In such cases, visual observations were made.

## RESULTS AND DISCUSSION

Some of the test results are shown in figures 4 to 7 as photographs of the smoke in the stream injected from a cylinder in crossflow. The calculated boundary-layer thicknesses varied from 0.041 to 0.049 centimeter at angular injection locations  $\theta$  of  $15^\circ$  to  $60^\circ$  from the stagnation line. The injected film was always thicker than the calculated boundary layer even at local blowing ratios  $M$  as low as 0.21 and for  $\theta$  as far as  $60^\circ$  from the stagnation line.

A top view of the air-smoke mixture being injected in the spanwise direction at a  $\beta$  of  $45^\circ$  is shown in figure 4. (The boundary-layer thickness is represented by the symbol  $\delta$ .) Photographic evidence and visual observations of the film injected at a  $\theta$  of  $15^\circ$  (fig. 4(a)) showed that the film remained close to the surface for an  $M_L$  of 1.18. Figure 4(b) shows the results of injection at a  $\theta$  of  $30^\circ$  for the same  $M_L$  of 1.18. The partially void area in the region immediately downstream of the exiting jet near the sur-

face indicates that the main bulk of the injected film had separated from the surface. Figure 4(c) shows that separation also occurred at a  $\theta$  of  $45^\circ$  even though the blowing ratio was lower ( $M_L = 0.86$ ). Figure 4(d) shows that an even greater film separation from the surface occurred at a  $\theta$  of  $60^\circ$  although the  $M_L$  was only 0.70. The same trend of increased film separation from the surface with increased  $\theta$  was observed at a  $\beta$  of  $30^\circ$ . This tendency of the film to separate from the surface with increased  $\theta$  would, in a turbine application, promote undesirable mixing with the hot mainstream and result in increased aerodynamic losses. It would also be expected to decrease the film-cooling effectiveness at a given  $M_L$ . Reference 3, however, shows an opposite trend with respect to film-cooling effectiveness. The reason is not known.

The effect of local blowing ratio at each of the two injection angles  $\beta$  ( $30^\circ$  and  $45^\circ$ ) at a fixed injection location  $\theta$  of  $30^\circ$  is shown in figure 5. At a low blowing ratio  $M_L$  of 0.38 and at a  $\beta$  of  $30^\circ$  (fig. 5(a)), the injected stream lay close to the surface in the injection area. When the film reached a  $\theta$  about  $60^\circ$  from the stagnation line, it unexpectedly separated from the surface. This is not consistent with other observations (fig. 5(d), e.g.), and the reason is not apparent. At a higher  $M_L$  of 0.59 (fig. 5(b)), the film was thicker but was still close to the surface in the injection area. As the  $M_L$  was increased to 1.18 (fig. 5(c)), the film separated from the surface soon after injection. This figure is an example of the photographic difficulty sometimes encountered. The void area does not appear clearly because of light reflections. An auxiliary figure (fig. 6) shows injection at the same conditions as figure 5(c) but with overhead lighting. The void area can be more clearly seen.

From these results, we would expect that the cooling effectiveness just downstream of the holes would increase with blowing ratio, reach a maximum between  $M_L = 0.59$  and  $M_L = 1.18$ , and then start to decrease as the blowing ratio was further increased. These results agree with the heat-transfer measurements on a cylinder (ref. 3), which showed that maximum cooling effectiveness occurred at a blowing ratio of about 1. These results, however, disagreed with heat-transfer measurements on a rounded-leading-edge, flat-plate model (ref. 4), which showed that the maximum cooling effectiveness immediately downstream of the holes on the leading edge occurred at blowing ratios between 0.4 and 0.5. The reason for the difference may be the different geometries of the models tested.

As figures 5(d) to (f) show, the results with a  $\beta$  of  $45^\circ$  were the same as those with a  $\beta$  of  $30^\circ$ , except that the film thicknesses were greater for  $45^\circ$  injection than for  $30^\circ$  injection. This means that, for a film-cooled turbine vane, more of the film would lie close to the surface with  $30^\circ$  injection. This should produce more effective wall cooling. This result agrees with the heat-transfer results of reference 3, which showed an improvement in film-cooling effectiveness with decreasing  $\beta$ .

Another important factor influencing film cooling is the lateral (spanwise) spreading and coverage of the surface. At blowing ratios above about 0.4, visual observation of film injection at all angular locations  $\theta$  showed no observable difference in the width (or spreading) from the injection point to about  $80^\circ$  from the stagnation line. At blowing ratios below 0.40 the injected stream "necked down" slightly about two hole diameters downstream. Figure 7 is a side view of film injection from a  $\theta$  of  $30^\circ$ . This figure illustrates how much the film spread and its deflection from the streamwise direction as it flowed over the cylinder surface. The photographic results were adversely affected by light reflections. Three blowing ratios are illustrated ( $M_L$  of 0.38, 0.60, and 1.19). Figure 7(a) shows the cylinder with no injection and is included to establish the location of the stagnation line. At an  $M_L$  of 0.38 (fig. 7(b)), no spreading can be seen. Although it is not shown clearly in the photograph, there was, as mentioned previously, a slight necking down of the film stream at about two hole diameters downstream. The injected film was almost immediately turned in a direction nearly parallel to the mainstream. At an  $M_L$  of 0.60 (fig. 7(c)) the nearly constant width of the film stream was maintained. At the hole exit, this film was inclined at an angle of approximately  $25^\circ$  to the mainstream. Within one hole diameter downstream of injection, the film was bent to about  $5^\circ$  from the mainstream. When the blowing ratio was increased to 1.19 (fig. 7(d)), the film was inclined at an angle of approximately  $35^\circ$  to the mainstream at the hole exit. Within one hole diameter downstream of injection, the film was bent to about  $10^\circ$  from the mainstream. Generally, for the cylinder, the absence of film spreading and the small lateral angles of the injected stream indicate difficulty in obtaining good lateral coverage even when the film-cooling air is injected in a spanwise direction.

From these results, we would expect the cooling effectiveness to remain highest in the mainstream direction downstream of the holes. Reference 3, however, showed that lower cooling effectiveness was measured in this region than between the holes. This would indicate that some deflection and spreading of the film occurred in the tests of reference 3. The reason for this difference in results may be the three times larger cylinder-diameter-to-cooling-hole-diameter ratio used in reference 3 than used herein. The cylinder-diameter-to-cooling-hole-diameter ratio of 10.47 used herein was representative of that expected in advanced turbine vanes.

## SUMMARY OF RESULTS

This investigation provided insight, by means of flow visualization, into the fluid mechanics encountered when film air is injected spanwise through a row of holes in a cylinder surface in crossflow. The cylinder simulated a film-cooled, advanced-turbine-vane leading edge. The results were as follows:



1. The injected film was always thicker than the calculated boundary layer even at local blowing ratios (ratios of injection-stream mass flux to local free-stream mass flux) as low as 0.21 and for injections as far as  $60^\circ$  from the stagnation line. As expected, increasing the blowing ratio resulted in more rapid growth of film thickness and a greater tendency for the film to separate from the surface.

2. Separation of the film from the surface occurred at lower blowing ratios as the film was injected at greater angles from the stagnation line. For example, separation occurred at a blowing ratio of 1.18 for injection at  $30^\circ$  from the stagnation line, at a ratio of 0.86 for injection at  $45^\circ$  from the stagnation line, and at a ratio of 0.70 for injection at  $60^\circ$  from the stagnation line.

3. Film thicknesses at a given blowing ratio were greater for injection at  $45^\circ$  to the surface than for injection at  $30^\circ$  to the surface.

4. At blowing ratios above about 0.4 there was no observable difference in the width (or spreading) of the injected stream from the injection point to about  $80^\circ$  from the stagnation line. This was observed for all injection locations. At blowing ratios below 0.4, the injected stream "necked down" slightly about two hole diameters downstream of injection.

5. At low blowing ratios (below about 0.4), the injectant was turned almost immediately in a direction nearly parallel to the mainstream. At high blowing ratios (above about 1.0) the flow at the hole exit was inclined at an angle of approximately  $35^\circ$  to the mainstream. The angle then decreased to about  $10^\circ$  to the mainstream within one hole diameter downstream of injection.

Lewis Research Center,  
National Aeronautics and Space Administration,  
Cleveland, Ohio, April 4, 1979,  
505-04.

#### REFERENCES

1. Moffitt, Thomas P.; Stepka, Francis S.; and Rohlik, Harold E.: Summary of NASA Aerodynamic and Heat Transfer Studies in Turbine Vanes and Blades. NASA TM X-73518, 1976.
2. Gauntner, James W.: Effects of Film Injection Angle on Turbine Vane Cooling. NASA TP-1095, 1977.
3. Luckey, D. W.; et al.: Stagnation Region Gas Film Cooling for Turbine Blade Leading Edge Applications. AIAA Paper 76-728, July 1976.

4. Sasaki, Makoto; et al.: Study on Film Cooling of Turbine Blades. Bull. Jap. Soc. Mech. Eng., vol. 19, no. 137, Nov. 1976, pp. 1344-1352.
5. Colladay, Raymond S.; and Russell, Louis M.: Streakline Flow Visualization of Discrete-Hole Film Cooling with Normal, Slanted, and Compound Angle Injection. NASA TN D-8248, 1976.
6. Schlichting, Herman (J. Kestin, transl.): Boundary-Layer Theory. Sixth ed. McGraw-Hill Book Co., Inc., 1968.

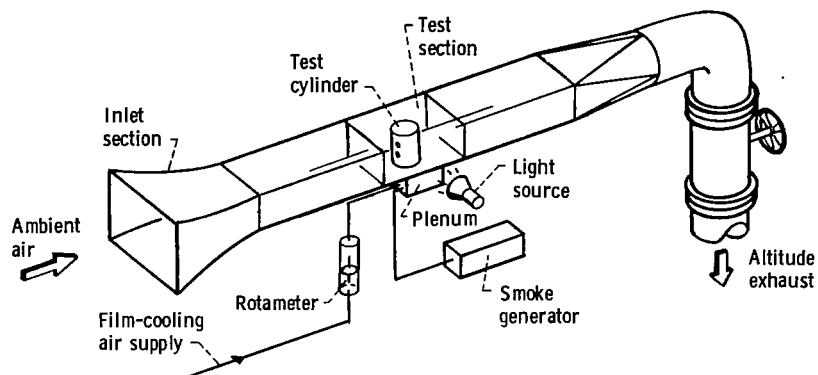


Figure 1. - Film-cooling flow-visualization facility.

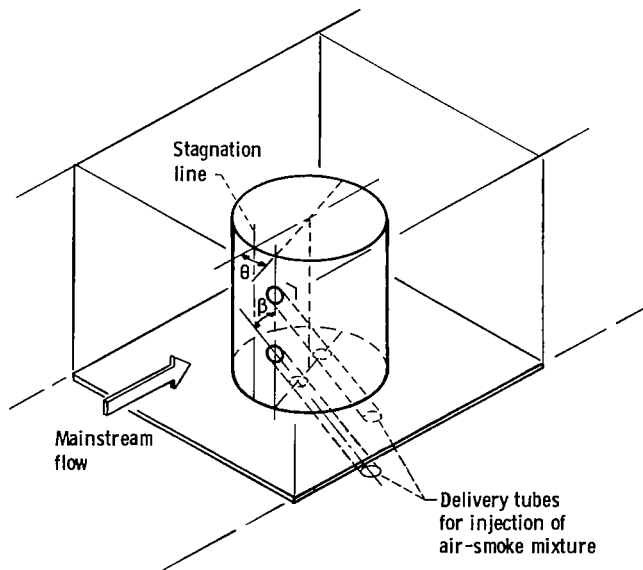


Figure 2. - Test section, where  $\beta$  is the injection angle relative to the surface and  $\theta$  is the angular location from the stagnation line.

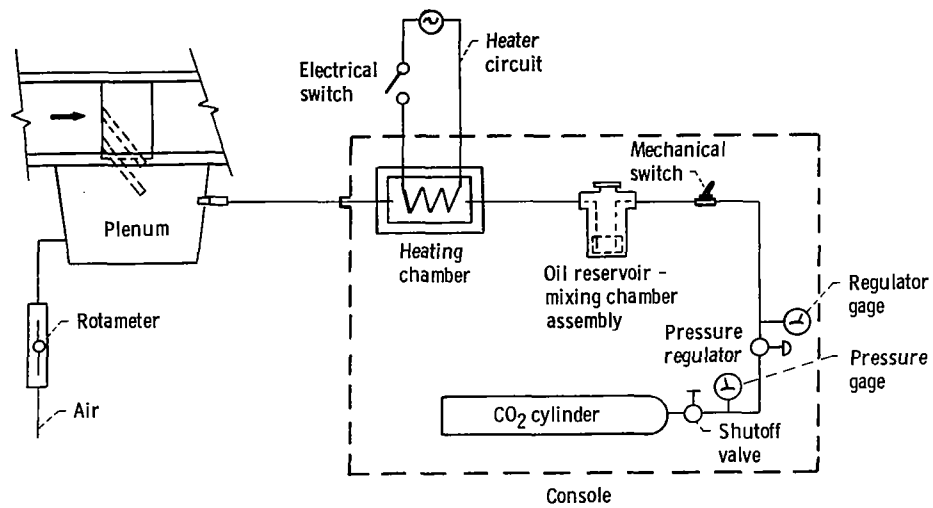


Figure 3. - Smoke generator.

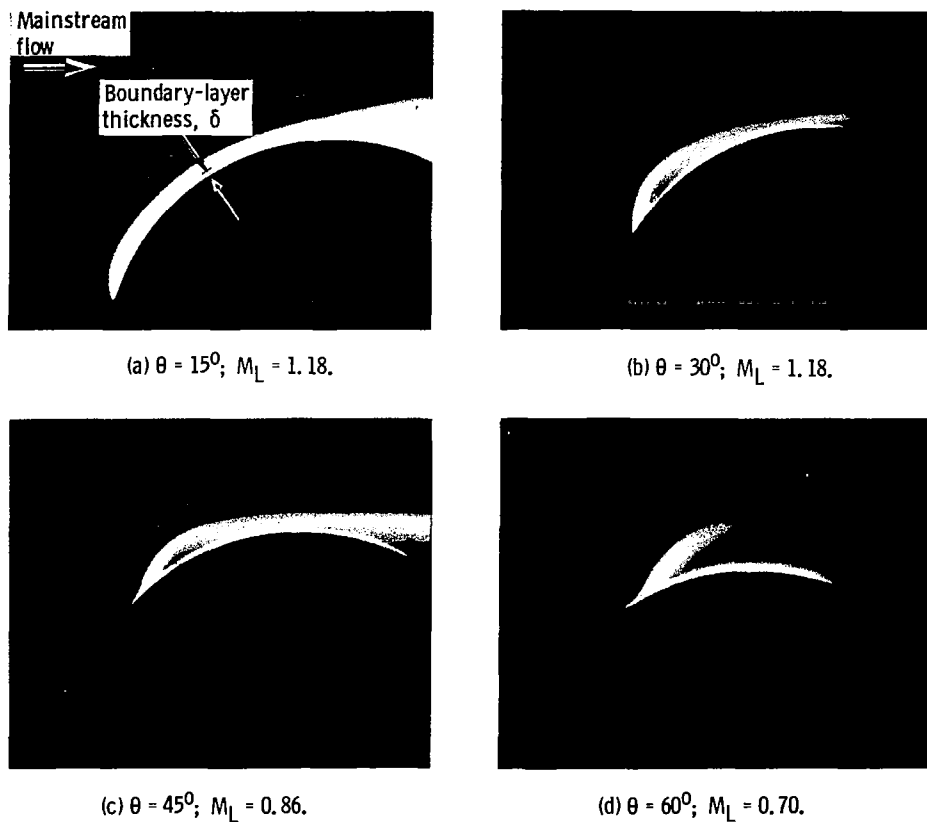
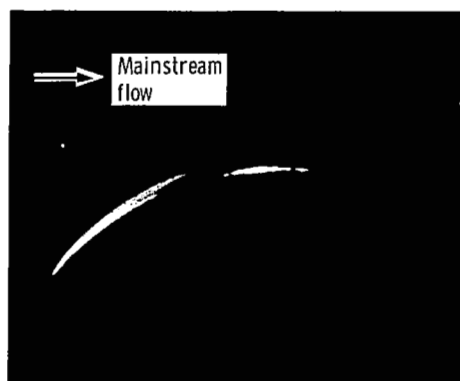
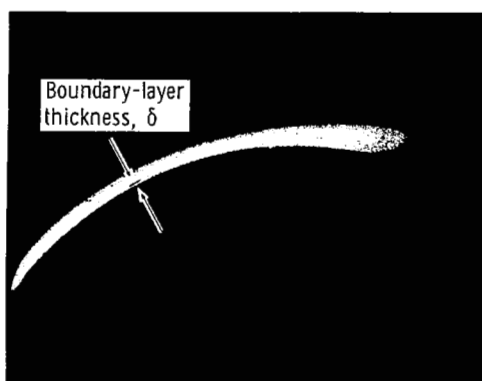


Figure 4. - Effect of film injection location  $\theta$  on a cylinder in crossflow at selected local blowing ratios  $M_L$ . Injection angle  $\beta$ ,  $45^\circ$ .



(a)  $\beta = 30^\circ$ ;  $M_L = 0.38$ .



(b)  $\beta = 30^\circ$ ;  $M_L = 0.59$ .



(c)  $\beta = 30^\circ$ ;  $M_L = 1.18$ .



(d)  $\beta = 45^\circ$ ;  $M_L = 0.37$ .



(e)  $\beta = 45^\circ$ ;  $M_L = 0.59$ .



(f)  $\beta = 45^\circ$ ;  $M_L = 1.18$ .

Figure 5. - Effect of local blowing ratio  $M_L$  and injection angle  $\beta$  on a cylinder in crossflow. Injection location,  $\theta$ ,  $30^\circ$ .

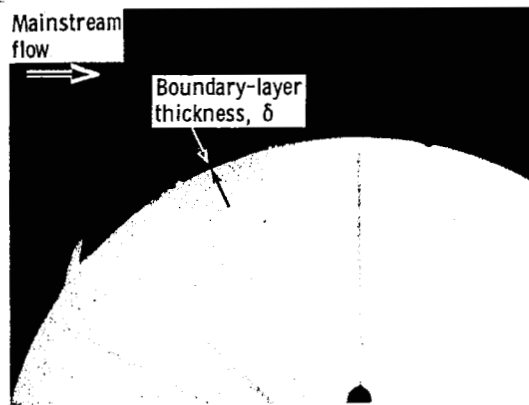
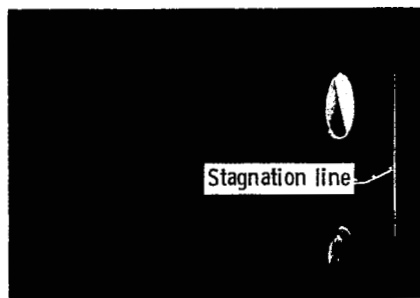
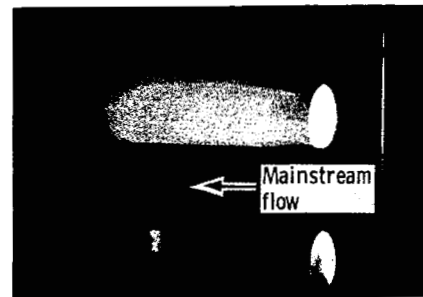


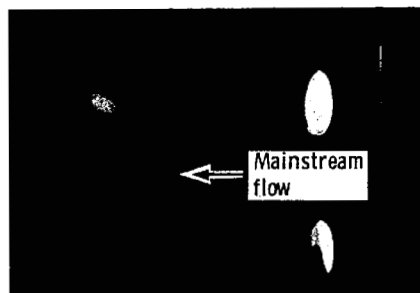
Figure 6. - Film injection at  $\beta = 30^\circ$ ,  $M_L = 1.18$ , and  $\theta = 30^\circ$ . (Same conditions as fig. 5(c).)



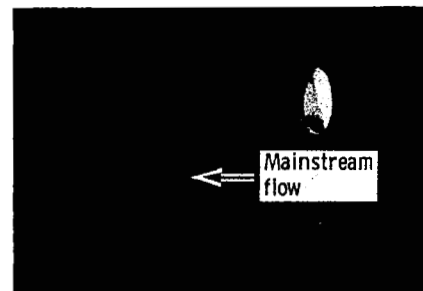
(a) Reference (no flow).



(b)  $M_L = 0.38$ .



(c)  $M_L = 0.60$ .



(d)  $M_L = 1.19$  (injection through upper hole only).

Figure 7. - Side view of injected film from a cylinder in crossflow, at various blowing ratios. Spanwise holes; injection angle,  $\beta$ ,  $30^\circ$ ; injection location,  $\theta$ ,  $30^\circ$ .

1. Report No. <b>NASA TP-1491</b>	2. Government Accession No.	3. Recipient's Catalog No.	
4. Title and Subtitle <b>FLOW VISUALIZATION OF DISCRETE-HOLE FILM COOLING WITH SPANWISE INJECTION OVER A CYLINDER</b>		5. Report Date July 1979	
		6. Performing Organization Code	
7. Author(s) <b>Louis M. Russell</b>		8. Performing Organization Report No. <b>E-9946</b>	
		10. Work Unit No. <b>505-04</b>	
9. Performing Organization Name and Address <b>National Aeronautics and Space Administration Lewis Research Center Cleveland, Ohio 44135</b>		11. Contract or Grant No.	
		13. Type of Report and Period Covered <b>Technical Paper</b>	
12. Sponsoring Agency Name and Address <b>National Aeronautics and Space Administration Washington, D. C. 20546</b>		14. Sponsoring Agency Code	
15. Supplementary Notes			
16. Abstract  An investigation was conducted to provide insight into the fluid mechanics encountered when film air from a single row of holes is injected over a cylinder in a mainstream at conditions simulating a film-cooled, turbine-vane leading edge. Smoke was added to the cooling air to visualize its flow path. Film was injected in the spanwise direction at angles of 30° and 45° to the surface; at angular locations of 15°, 30°, 45°, and 60° from the stagnation line; and at various blowing ratios. The observations were related to the measured heat-transfer data of others.			
17. Key Words (Suggested by Author(s))  <b>Turbine cooling Film cooling Flow visualization</b>		18. Distribution Statement  <b>Unclassified - unlimited STAR Category 07</b>	
19. Security Classif. (of this report) <b>Unclassified</b>	20. Security Classif. (of this page) <b>Unclassified</b>	21. No. of Pages <b>14</b>	22. Price* <b>A02</b>